



**UNSW**  
THE UNIVERSITY OF NEW SOUTH WALES  
SYDNEY • AUSTRALIA

## Real Time CRDS Spectroscopy

### The Opportunity

Cavity Ring Down Spectroscopy (CRDS) is a highly sensitive spectroscopic technique for measurement and analysis of a sample by the scatter and absorption of light. It is widely used to identify the presence of analytes in gaseous samples down to the parts per trillion level. While CRDS is very sensitive, it is commonly hindered by the ability to rapidly extract information from complex absorption data. A new Fourier-transform based signal processing method developed at UNSW@ADFA overcomes the performance limitations of existing methods affording real time analysis. This increase in processing performance increases the versatility of CRDS for a number of applications.

The technology can be used with pulsed and CW laser sources, and is specifically suited to the new quantum cascade lasers (QCL). Figure 1 shows pressure scans at two pulsed QCL wavelengths, and illustrates that this technology can be used to monitor the gas species over a very large pressure range.

The technology can be used in conjunction with CRDS as well as well established techniques such as Fourier-Transform Infra-Red (FTIR) spectroscopy instruments to rapidly extract absorbance data from tens to hundreds of absorption features in a single spectrum. This approach can be added to existing FTIR spectrometers and does not alter the data collection process. For some spectral features, quantitative absorbance data may be obtained without the need of a background scan.

### The Team

The technology was developed by A.Prof. Charles Harb and his team at UNSW@ADFA. NewSouth Innovations Pty Limited (NSi) is responsible for the knowledge exchange and commercialisation of research and technologies developed at UNSW

### Investment Opportunity

NSi is seeking licensees to take the technology to market. The technology is currently subject to a Patent Cooperation Treaty (PCT) application. If more detailed information is required, this can be provided under a confidentiality agreement.

### Find out more

Please contact Dr Tim Boyle, Business Development Manager, NewSouth Innovations  
t.boyle@nsinnovations.com.au | Tel: +61 2 9385 9762

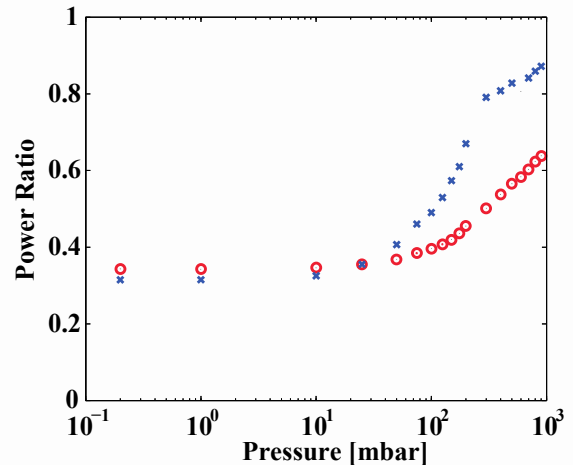


**Figure 1.** Room air measurements at 6000nm (blue x) and 6100nm (red o).

## Contact NewSouth Innovations



NewSouth  
Innovations

**NewSouth Innovations Pty Limited**

University of New South Wales, Sydney, Australia

Enquiries: [info@nsinnovations.com.au](mailto:info@nsinnovations.com.au)

T: +61 2 9385 5008

[www.nsinnovations.com.au](http://www.nsinnovations.com.au)

## **FAQ: UNSW Cavity Ring Down Spectroscopy Technologies**

- 1. What are the potential applications for the technology?**
  - a. The technology can be used for quality control in food preparation quality control, isotope ratio measurement, process control monitoring and environmental monitoring. There has been significant interest in airport security applications from organisations such as US Homeland Security, Australian Federal Police and ASIO.
- 2. What are the key performance benefits?**
  - a. The technology is up to 1000 times more sensitive than existing approaches. It also can process the information at up to 500 times faster.
- 3. What is the current IP position?**
  - a. The processing method and apparatus is currently subject to a Patent Cooperation Treaty (PCT) application. This method is applicable to CRDS instruments and existing FTIR systems. The team have also developed an optimised CRDS instrument which is currently protected by trade secret.
- 4. What are the innovative features of the opportunity?**
  - a. New data extraction options which can be used for CRDS or existing FTIR systems. The optimised CWCRDS apparatus also lends itself to security applications due to its size and scale which are portable.
- 5. What is the investment opportunity? What is UNSW Seeking?**
  - a. UNSW and NSi are seeking a collaborative research agreement to finalise the offering and/or a license agreement to convert the invention to a prototype product.
- 6. What advantage does the technology offer over existing and alternative technologies available?**
  - a. This technology lends itself to miniaturization and the use of specialty laser sources that can be wavelength scanned rapidly. As also mentioned above, the processing method also allows rapid measurement of analytes at extremely low concentrations.
- 7. How can the technology be implemented for chemical analysis?**
  - a. We have recently completed research which demonstrates analysis of several chemical species. We are currently drafting a journal article which will highlight the utility of the technology.
- 8. Details of liquid phase work if available?**
  - a. To date we have been concentrating on gas phase measurements due to the interest from the security sector, but liquid phase determinations should be possible with slight modifications.

# Frequency domain analysis for laser-locked cavity ringdown spectroscopy

T. K. Boyson,<sup>1</sup> T. G. Spence,<sup>2</sup> M. E Calzada,<sup>3</sup> and C. C. Harb<sup>1</sup>

<sup>1</sup>*School of Engineering and Information Technology, University College, The University of New South Wales, Canberra, ACT, 2600, Australia*

<sup>2</sup>*Department of Chemistry, Loyola University New Orleans, New Orleans, Louisiana 70118, USA*

<sup>3</sup>*Department of Mathematics, Loyola University New Orleans, New Orleans, Louisiana 70118, USA*

[\\*tkboyson@gmail.com](mailto:tkboyson@gmail.com)

**Abstract:** In this paper we report on the development of a Fourier-transform based signal processing method for laser-locked Continuous Wave Cavity Ringdown Spectroscopy (CWCARDS). Rather than analysing single ringdowns, as is the norm in traditional methods, we amplitude modulate the incident light, and analyse the entire waveform output of the optical cavity; our method has more in common with Cavity Attenuated Phase Shift Spectroscopy than with traditional data analysis methods. We have compared our method to Levenburg-Marquardt non linear least squares fitting, and have found that, for signals with a noise level typical of that from a locked CWCARDS instrument, our method has a comparable accuracy and comparable or higher precision. Moreover, the analysis time is approximately 500 times faster (normalised to the same number of time domain points). Our method allows us to analyse any number of periods of the ringdown waveform at once: this allows the method to be optimised for speed and precision for a given spectrometer.

© 2011 Optical Society of America

**OCIS codes:** (280.3420) Laser sensors; (120.6200) Spectrometers and spectroscopic instrumentation.

---

## References and links

1. S. M Ball, I. M. Povey, E. G. Norton, and R. L. Jones, "Broadband cavity ringdown spectroscopy of the NO<sub>3</sub> radical," *Chem. Phys. Lett.* **342**, 113–120 (2001).
2. J. Xie, B. A. Paldus, E. H. Wahl, J. Martin, T. G. Owano, C. H. Kruger, J. S. Harris, and R. N. Zare, "Near-infrared cavity ringdown spectroscopy of water vapor in an atmospheric flame," *Chem. Phys. Lett.* **284**(5), 387–395 (1998).
3. A. O'Keefe and D. A. G. Deacon, "Cavity ring-down optical spectrometer for absorption measurements using pulsed laser sources," *Rev. Sci. Instrum.* **59**, 2544–2551 (1988).
4. A. A. Istratov and O. F. Vyvenko, "Exponential analysis in physical phenomena," *Rev. Sci. Instrum.* **70**(2), 1233–1257 (1999).
5. T. G. Spence, C. C. Harb, B. A. Paldus, R. N. Zare, B. Wilke, and R. L. Byer, "A laser-locked cavity ring-down spectrometer employing an analog detection scheme," *Rev. Sci. Instrum.* **71**(2), 347–353 (2000).
6. P. D. Kirchner, W. J. Schaff, G. N. Maracas, L. F. Eastman, T. I. Chappell, and C. M. Ransom, "The analysis of exponential and nonexponential transients in deep level transient spectroscopy," *J. Appl. Phys.* **52**, 6462–6470 (1981).

7. M. Mazurenka, R. Wada, A. J. L. Shillings, T. J. A. Butler, J. M. Beames, and A. J. Orr-Ewing, "Fast Fourier transform analysis in cavity ring-down spectroscopy: application to an optical detector for atmospheric NO<sub>2</sub>," *Appl. Phys. B* **81**, 135–141 (2005).
8. M. A. Everest and D. B. Atkinson, "Discrete sums for the rapid determination of exponential decay constants," *Rev. Sci. Instrum.* **79**, 023108 (2008).
9. D. Halmer, G. von Basum, P. Hering, and M. Murtz, "Fast exponential fitting algorithm for real-time instrumental use," *Rev. Sci. Instrum.* **75**, 2187 (2004).
10. R. Engeln, G. von Helden, G. Berden, and G. Meijer, "Phase shift cavity ring down absorption spectroscopy," *Chem. Phys. Lett.* **262**, 105–109 (1996).
11. R. W. P. Drever, J. L. Hall, F. Kowalski, J. Hough, G. M. Ford, A. J. Munley, and H. Ward, "Laser phase and frequency stabilization using an optical resonator," *Appl. Phys. B: Photophys. Laser Chem.* **31**, 97–105 (1983).
12. S. Z. Sayed Hassen, M. Heurs, E. H. Huntington, I. R. Petersen, and M. R. James, "Frequency locking of an optical cavity using linear quadratic Gaussian integral control," *J. Phys. B* **42**(17), 175501 (2009).
13. B. A. Paldus, C. C. Harb, T. G. Spence, B. Wilke, J. Xie, J. S. Harris, and R. N. Zare, "Cavity-locked ring-down spectroscopy," *J. Appl. Phys.* **83**(8), 3991–3997 (1998).
14. P. Zalicki and R. N. Zare, "Cavity ring-down spectroscopy for quantitative absorption measurements," *J. Chem. Phys.* **102**, 2708–2717 (1995).

## 1. Introduction

Cavity ringdown spectroscopy (CRDS) is a sensitive spectroscopic technique that can be used to measure absorption due to weakly absorbing or dilute samples. In a CRDS measurement, light (generally this is from a laser, but broadband techniques have been demonstrated. e.g. [1]) is coupled into an optical cavity formed by two or more mirrors. Upon extinguishing the incident light, the field within the cavity,  $I(t)$ , decays according to:

$$I(t) = \alpha e^{\left(\frac{-t}{\tau}\right)} + b \quad (1)$$

where  $\alpha$  is the initial intensity,  $t$  is time,  $b$  is an offset, and  $\tau$  is the decay length (the time taken for the field to decay to  $\frac{1}{e}$  of its initial value). The decay length is a direct measure of the losses within the cavity, comprising of the reflectivity of the mirrors, a lumped term due to scattering and other small losses, and the loss due to an absorbing species in the cavity.  $\tau$  may be thus quantified:

$$\tau = \frac{T_{rt}}{(\varepsilon(\lambda)c + n(1 - R) + A)} \quad (2)$$

where:  $T_{rt}$  is the roundtrip time for light in the cavity,  $\varepsilon(\lambda)$  is the extinction coefficient (as a function of wavelength,  $\lambda$ ) of an absorbing species with concentration  $c$ ;  $n$  is the number of mirrors with reflectivity  $R$ ; and  $A$  is a lumped term comprising of all other absorptions (such as scattering, and absorption at the surface of the mirrors). An absorption spectrum is generated by scanning the frequency of the incident light while recording the decay length. These measurements are scaled by a measurement of the empty cavity decay length,  $\tau_0$ . Traditional data processing techniques rely on fitting the exponential decay of the cavity field with a least squares algorithm [2]. If the logarithm of the decay is taken, linear least squares may be used [3]; else, a non-linear least squares fitting algorithm (such as Levenburg-Marquardt, LM) must be used. Linear least squares has the advantage that it returns a closed form solution requiring only a single iteration to complete; however, it is susceptible to noise, and requires that the baseline be determined and subtracted [3, 4]. Non linear least squares must find the solution iteratively (each iteration requires a linear least squares fit). If it is required to fit all three parameters of the decay, it is slow (fitting an exponential in Matlab, for example, takes several ms to fit a 1000 point decay). Moreover, LM requires the operator (or computer) to make an initial guess of the fit parameters; a poor guess may result in the algorithm diverging from the solution, or taking an infinite amount of time to converge on a solution [4]. CRDS was originally developed

with pulsed lasers [3]: at a pulse repetition rate of 20Hz, a least squares fitting regime may be fast enough to keep up with instrumental output; systems using CW lasers and a fast optical switch, however, may generate transients at rates exceeding 50kHz [5]. The problem of fitting an isolated exponential decay rapidly and accurately is not unique to CRDS. Indeed, the fitting of exponential decays is a fundamental problem of applied signal processing. Istratov and Vyvenko [4] comprehensively outline the available solutions to this problem. They conclude that, when considering speed, precision, and ease of implementation, a method based on the Fourier transform of the decay developed by Kirchner *et al.* [6] for deep transient level spectroscopy, and adapted by Mazurenka *et al.* [7] for CRDS was the best solution. Everest *et al.* [8] analysed the methodology of Mazurenka and found systematic errors in the derivation of equations resulting from the assumption that the data were continuous rather than discrete. Everest compared the correct Fourier transform method with an improved method based on that published by Halmer *et al.* [9] based upon corrected successive integration (CSI); both The FT and CSI methods were found to be significantly faster than LM, but with a comparable accuracy. All of these methods rely on building up light inside of the cavity, then capturing a single decay transient for analysis. Here, we propose a new methodology for the extraction of  $\tau$  from the ringdown cavity. Our method has more in common with Phase-Shift CRDS (otherwise known as Cavity Attenuated Phase Shift Spectroscopy, or CAPS) [10] than it does with traditional fitting methods: rather than considering only the exponential decay of the cavity to either a pulse or a sudden shuttering of the input light and analysing a single decay, we consider the response of the cavity to an amplitude modulated field, and analyse the output as a whole. Not only is this fast, it makes acquisition electronics much easier to design. In this paper we will first outline the theory for our new technique. We will then give details of a comparison of our technique to Levenburg-Marquardt fitting with simulated data. We will then give details of the experimental setup that we have used for proof of concept test. We then give our conclusions, and details of where we hope to implement this new data processing technique.

## 2. Theoretical description of the CRDS system

Consider the impulse response of the cavity:

$$I(t) = \alpha \exp\left(\frac{-t}{\tau}\right) \quad (3)$$

This equation (and the following mathematics) may be extended to a multi-exponential decay, but here we only consider the case for a cavity modelocked to the incident laser light; such a setup is almost guaranteed to return a single decay (presuming that the detection electronics have been designed with enough bandwidth). By taking the Fourier transform of Eq. (3), we can generate the frequency response ( $F(\omega)$ ) of the cavity to an input at angular frequency  $\omega$ :

$$F(\omega) = \int_0^{\infty} I(t) e^{-j\omega t} dt \quad (4)$$

Thus:

$$F(\omega) = \frac{\alpha \tau}{\tau \omega j + 1} \quad (5)$$

$F(\omega)$  may be broken into real and imaginary parts:

$$\Re(F(\omega)) = \frac{\alpha \tau}{\omega^2 \tau^2 + 1} \quad (6)$$

$$\Im(F(\omega)) = -\frac{\omega\alpha\tau^2}{\omega^2\tau^2 + 1} \quad (7)$$

These two equations, respectively, are the response of the cavity to a cosine and sine of frequency  $\omega$ ; equivalently, they are the real and imaginary components of the Fourier transform. Here, we will only consider the case of cosine, *i.e.* the real part of the Fourier transform, although an analogous formalism may be developed for sine. Consider measuring the response of the cavity to two frequencies, with one being equal to some frequency multiple,  $a$ , of the other *i.e.*  $\omega$  and  $a\omega$ , then we find:

$$\Re(F(\omega)) = \frac{\alpha\tau}{\omega^2\tau^2 + 1} \quad (8)$$

$$\Re(F(a\omega)) = \frac{\alpha\tau}{(a\omega)^2\tau^2 + 1} \quad (9)$$

If we take the ratio of these, we find:

$$\frac{\Re(F(\omega))}{\Re(F(a\omega))} = \frac{a^2\omega^2\tau^2 + 1}{\omega^2\tau^2 + 1} \quad (10)$$

and then by rearranging for  $\tau$ , we obtain:

$$\tau = \frac{1}{\omega} \sqrt{\frac{1-P}{P-a^2}} \quad (11)$$

where  $P = \frac{\Re(F(\omega))}{\Re(F(a\omega))}$ ; the ratio of the magnitudes of two peaks in frequency space. Thus, by calculating the ratio of the magnitudes of two peaks in frequency space, we can easily calculate  $\tau$ . A measurement for  $\tau$  can be obtained, for example, by modulating the light at  $\omega$ , measuring the system response, then modulating at  $a\omega$  and taking the ratio. Alternatively, and more conveniently, we could choose to use a square-wave-modulated light source (*i.e.* rapidly switched on and off) with a 50% duty cycle incident on the cavity. The Fourier series for a square wave,  $s(t)$ , is given by:

$$s(t) = \frac{4}{\pi} \sum_{n=1,3,5,\dots}^{\infty} \frac{1}{n} \sin\left(\frac{n\pi t}{L}\right) \quad (12)$$

It can thus be seen that a square-wave modulated field has frequency components at  $f$ ,  $3f$ ,  $5f$ , *etc.*. The response of a locked cavity to squarewave modulate light is shown in Fig. 1. Due to the orthogonality of the sinusoids, we can analyse each of these components separately; we can thus calculate  $\tau$  from a single measurement. Practically, we use the fundamental and the first harmonic, as the signal-to-noise is highest. For the case outlined above,  $\tau$  is given by:

$$\tau = \frac{1}{\omega} \sqrt{\frac{1-P}{P-9}} \quad (13)$$

In order to measure the response at each frequency of interest, we can of course calculate the discrete fourier transform (DFT) and measure the magnitude of the real peak, however, this is computationally wasteful as we are only interested in the value for two frequencies. Instead of evaluating the whole DFT:

$$F(\omega) = \sum_{n=0}^{N-1} f[n] e^{i\frac{2\pi jnk}{N}}, k = 0, 1, 2, \dots, N-1 \quad (14)$$

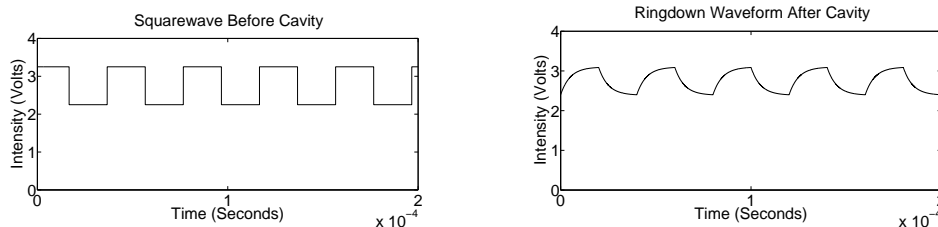


Fig. 1. Simulated 25 kHz squarewave and ringdown waveforms used to analyse and extract  $\tau$ . The squarewave is the light before the cavity; the ringdown waveform is the light after passing through a cavity with a decay time of  $5\mu s$ .

where  $k$  is the frequency in samples, and  $f[n]$  is the sampled time domain waveform. We evaluate it only at the frequencies of interest, e.g. for  $k = 1$ :

$$F(\omega) = \sum_{n=0}^{N-1} f[n]e^{j\frac{2\pi n}{N}\omega} \quad (15)$$

As we are only interested in the real part (the projection onto cosine), we do not need to evaluate the whole complex sum: we simply multiply the time-domain waveform by a cosine at the frequency of interest, and sum over  $n$ , for  $k = 1$ :

$$\Re(\omega) = \sum_{n=0}^{N-1} f[n]\cos\left(\frac{2\pi n}{N}\omega\right) \quad (16)$$

The DFT maps a set of  $N$  time domain data points onto a set of  $N$  frequency domain points, running from  $0, 1, \dots, N - 1$ : these frequency domain points are evenly spaced from 0 to the sampling frequency. As such, there is no guarantee that a given point (say, the maximum of a sharp spectral feature) will be included in the output. The information, however is still present. We can thus, rather than calculating the DFT by definition (*i.e.* by choosing an integer value of  $k$ ), we can choose our local oscillator (LO) frequency to sit precisely where the SNR is highest. Thus for a LO frequency  $\omega$ , where  $\omega$  may correspond to an integer value of  $k$ , but is not restricted to it:

$$\Re(\omega) = \sum_{n=0}^{N-1} f[n]\cos(\omega n) \quad (17)$$

This is identical to a digital mixer, or, if we evaluated a continuous integral rather than the discrete sum, a lock-in amplifier. In CAPS, the value of  $\omega$  is chosen such that  $\omega = \frac{1}{\tau}$  [10]. This maximises the change in the phase shift as a function of  $\tau$ . For our fourier method, the best modulation frequency would probably be where  $a\omega = \frac{1}{\tau}$ : this would result in the fundamental being essentially unattenuated by the cavity, while the first harmonic's attenuation would vary strongly as a function of  $\tau$ . For our system, with  $\tau_0 = 5\mu s$ , this would correspond to a modulation frequency of approximately 10 kHz; however, instrumental limitations prevent us from modulating this slowly, so we have chosen to work as slowly as we can, at 25 kHz.

### 3. Simulations

In order to test our frequency domain method, we have made a comparison to LM fitting in Matlab. Although there are other methodologies outlined in the literature [4, 6–8], most published papers, and, to our knowledge, all commercial instruments still use LM. To compare

the precision of the two methods we have simulated a dataset consisting 10,000 ringups and ringdowns with a SNR of 40 dB. For our method, we broke the data up into sets consisting of 1-200 periods (and thus 500-10,000 individual datasets). Each waveform within a set was analysed, and the set of solutions used to construct the probability histograms in Figure 2. For the Levenburg-Marquardt fit, the ringups were discarded and each individual ringdown fit for initial amplitude, ringdown time, and offset; this set of 10,000 solutions was used to construct the probability histogram for the fitting method. The results in Fig. 2 show that our method has a comparable accuracy to LM fitting, and that the precision increases as the length of the analysed data increases. This is to be expected, as our method is based on taking a running average.

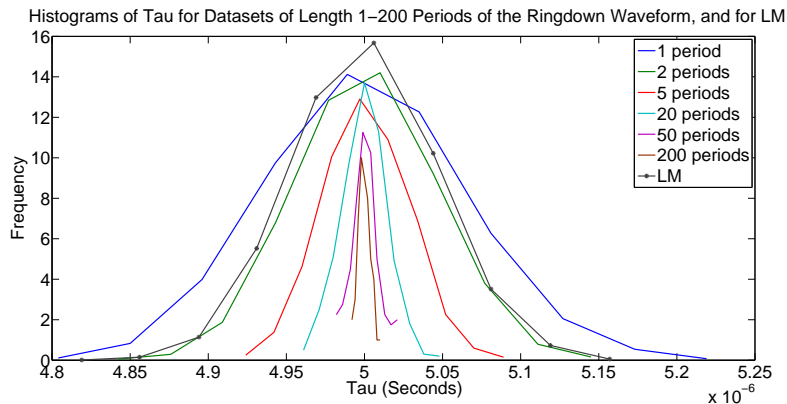


Fig. 2. Normalized histograms of Tau for various lengths of the ringdown waveform using our frequency domain method, and for Levenburg-Marquardt fitting. A sample waveform, consisting of 10,000 ringups and ringdowns, with a SNR of 40 dB was synthesised. For our method, the data were trimmed into various lengths, analysed, and the set of answers used to construct the probability histogram. For LM, the ringups were discarded, the ringdowns fit in Matlab, and the probability histogram generated from the set of answers. In reality, for our method, we would analyse the 10,000 period-long waveform as a whole, giving a single answer. This figure shows how the precision of our method increases with the length of the input data. All data lengths have a similar accuracy to LM, but for any length longer than 2 periods, our method has higher precision.

In order to further verify the performance of our fourier method, we have performed simulations that vary the number of periods analysed and the signal-to-noise of the waveform. For both of these simulations, we have simulated a ringdown waveform with 1000 periods (*i.e.* 1000 ringups and ringdowns); we have analysed single periods of the ringdown waveform with our fourier transform method, and discarded the ringups and analysed single ringdowns with LM fitting. The simulation for the data length vs. the ringdown time, Fig. 3, shows that our fourier method has a comparable precision and accuracy to LM fitting for all data lengths. The results in Fig. 4 show that, as per our simulations in Fig. 2, LM fitting gives a slightly higher, but comparable, precision to our FT method at all simulated noise levels. We note that the results are comparable for all of the simulated noise levels, even those well outside that expected from a locked CRDS spectrometer.

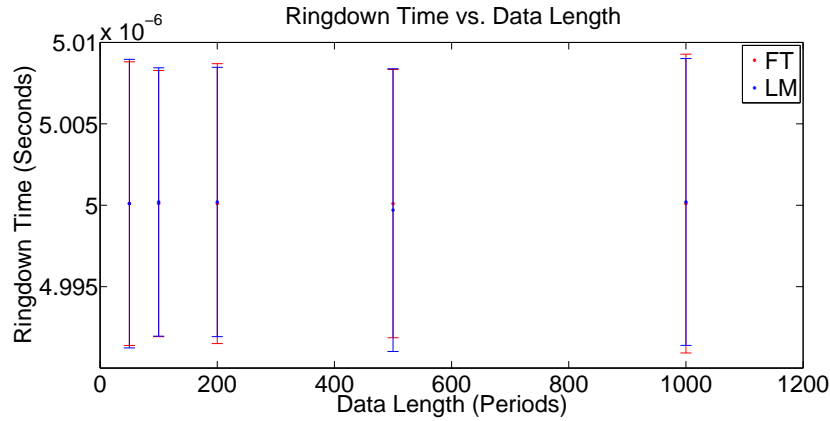


Fig. 3. Ringdown time vs. standard deviation for various numbers of periods analysed. This figure shows that our fourier method has a comparable precision and accuracy to LM fitting for all data lengths. The error bars represent one standard deviation.

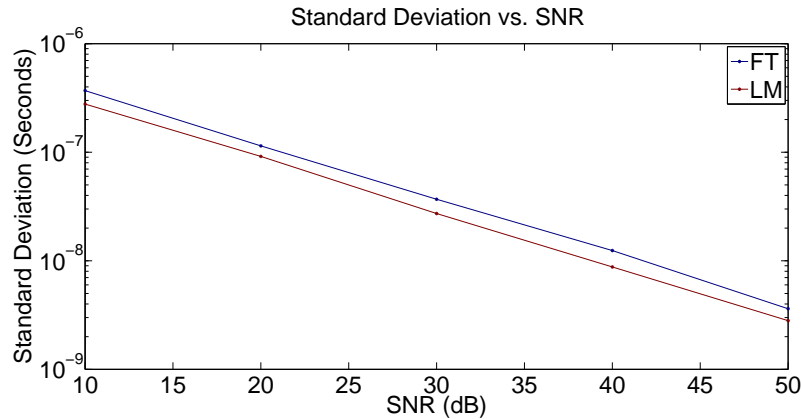


Fig. 4. Standard deviation vs. signal-to-noise for our fourier method, and for LM fitting.

#### 4. Experimental data

To confirm our simulation results, we have analysed a sample ringdown waveform from a CWCARDS instrument that we have built. A schematic diagram of the system is shown in Fig. 5. Briefly, light from an external cavity tunable diode laser (New Focus 6330, 10mW tunable from 1540-1640 nm) is passed through a Faraday isolator in order to prevent unwanted optical feedback. The light is then passed through an electro-optic modulator (EOM) (Thorlabs). The EOM places FM sidebands (at  $\pm 18$  MHz) on the laser radiation; these are used to lock the cavity to the laser using the method of Drever *et al.* [11]. The phase modulated light is then passed through an Acousto-Optic Modulator (AOM) (Brimrose) that is used to rapidly switch the laser light on and off (for this work, at 25kHz) in order to generate the waveform shown in Fig. 1. The light then passes through a polarising cube beamsplitter (PCB) and a quarter wave plate (QWP) before falling onto the optical cavity. The reflected beam passes back through the optical circulator, and is tapped off to lock the cavity. The cavity is a stainless steel tube (Los

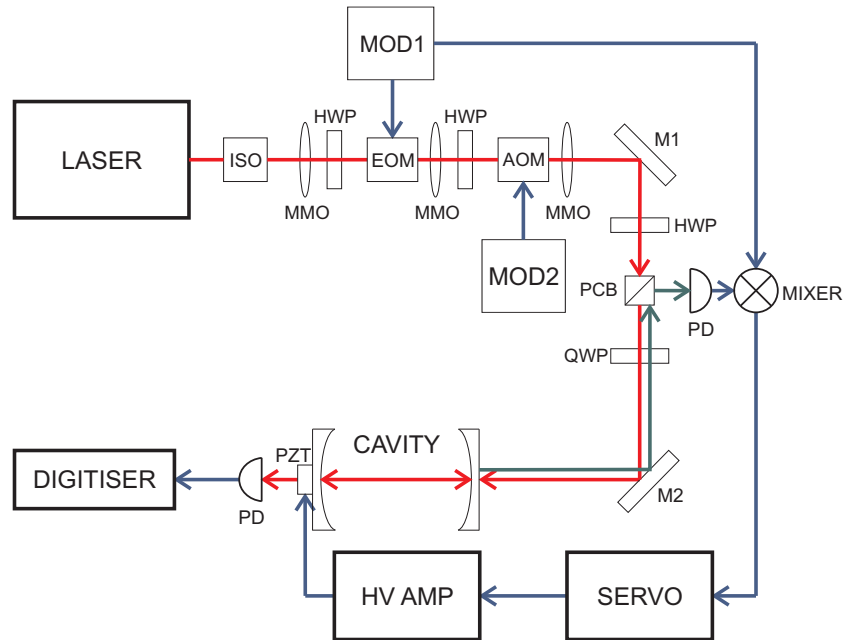


Fig. 5. Schematic diagram of laser-locked CRDS system. Abbreviations are as follows: ISO is the Faraday isolator; MMO are mode matching optics; HWP are half wave plates; EOM is the electro-optic modulator; AOM is the acousto-optic modulator; MOD1 is the RF generator and amplifier for phase modulation; MOD2 is the signal generator and amplifier used to generate the chopping waveform; M1 and M2 are beam steering mirrors; PCB is a polarizing cube beamsplitter; PD are photodetectors; QWP is a quarter wave plate; SERVO is the controller; HV AMP is a  $\pm 200V$  amplifier to drive PZT, the piezoelectric actuator that controls the cavity length.

Gatos Research) with a 99.96 % mirrors as both the input and output coupler (Advanced Thin Films,  $R > 99.96\%$ , loss  $< 10\text{ppm}$ ). These mirrors give a calculated empty cavity ringdown time of  $\approx 5\mu\text{s}$ . Both reflected and transmitted photodetectors were designed and built in house, they have a 3 dB bandwidth  $> 20\text{MHz}$ . The cavity is locked with an in house designed analog PI controller with a unity gain bandwidth of 1kHz. Light exiting the cavity is acquired using a high-speed digitising oscilloscope (Clevoscope 3284A, 100MS/sec, 14 bits), and exported to Matlab for analysis. A sample ringdown waveform from our instrument is shown in Fig. 6.

To test the theory above, 40 ms of data was taken and digitised on our Clevoscope 3284A with the full 14 bits, at a sampling frequency of 100 MHz. This resulted in the capture of 1000 ringups and ringdowns. For our FT method, the data were trimmed into various integer-number-of-period lengths, and then analysed as above. For the LM fits, the data were trimmed into individual ringdowns and analysed in Matlab. For our method,  $\tau$  was found to be  $5.521\mu\text{s}$ , with an analysis time of 720 msec to analyse the entire waveform as a single entity, and  $(5.522 \pm 0.151\mu\text{s})$  ( $\pm$  one standard deviation) with an analysis time 86.0 milliseconds to analyse the waveform as individual periods. For LM  $\tau$  was found to be  $(5.533 \pm 0.137\mu\text{s})$  ( $\pm$  one standard deviation), with an analysis time of 24.0 seconds. The analysis time for LM was found to be strongly dependant on the initial guesses for the fitting parameters; an initial guess of  $5\mu\text{s}$  for  $\tau$  led to the stated analysis time of 24.0 seconds, while an initial guess of  $1\mu\text{s}$  led to an analysis time of almost 45 seconds. The results from our analysis are shown in Fig. 7.

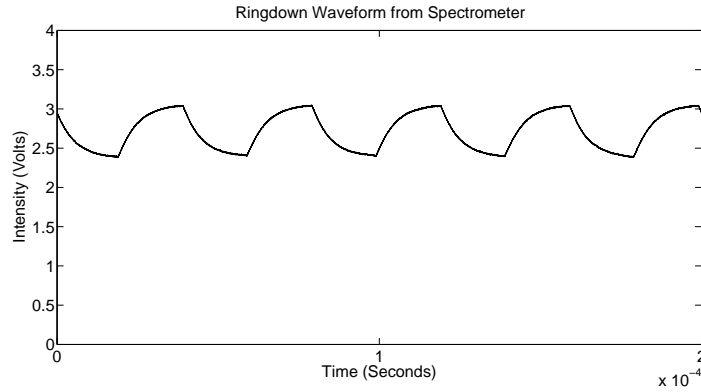


Fig. 6. 25 kHz CW Ringdown waveform, taken from our spectrometer. These are the data that we have analysed using our method and LM fitting.

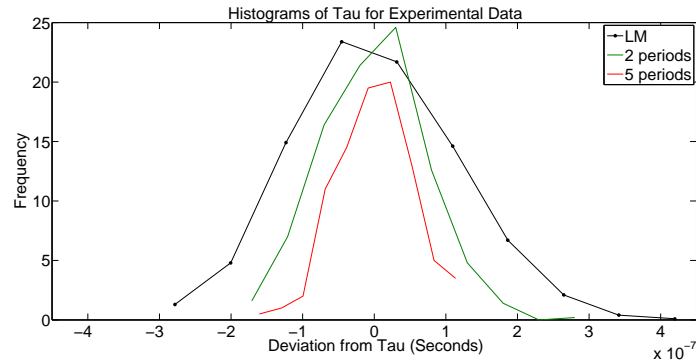


Fig. 7. Normalized histograms of Tau from experimental data. 40 ms of data at a 25 kHz chopping frequency were captured from our spectrometer. For our method, the data were chopped into lengths of 2 and 5 periods of the ringdown waveform, and the solutions used to construct the probability histogram. For LM, the ringups were discarded, the ringdowns fit using the aforementioned procedure, and the histogram constructed. It can be seen that our method has a comparable (but slightly higher) precision to LM for a waveform of 2 periods, and a higher precision for 5 periods. This supports our findings in the simulations we have performed. We have only analysed up to 5 periods here, as any longer data length does not give enough solutions for  $\tau$  to generate reliable statistics.

## 5. Discussion

In this paper, we have given a new method for analysing the output of a CWCRDS instrument. Rather than analysing single decay transients, we take advantage of the properties of our laser-locked spectrometer, and analyse the waveform at the output of the cavity as a whole. We find, in simulation, that our method has an accuracy comparable to Levenburg-Marquardt fitting (the defacto standard for CRDS) and a better precision for data similar to that from a CWCRDS instrument. We have built laser-locked CRDS instrument to perform proof of concept tests; experimentally, we find that the SNR at the frequencies we are analysing is comparable to that in our simulations:  $\approx 40\text{dB}$ . Our method was found to be more than 250 times faster at analysing

a dataset than LM; this increase in computational speed is in spite of the fact that our method analyses twice as much data as LM, as we analyse both the ringup and the ringdown. Because our method is based in the frequency domain, it is reasonably noise immune; the only noise that will affect the result is noise at the frequencies that we are analysing: as such we choose to work where the signal to noise ratio is highest. This may be compared to traditional fitting techniques, where noise at every frequency must be dealt with. Both our simulations and our experimental data were taken at a chopping frequency of 25 kHz and a sampling frequency of 100MHz; however, there is no reason not to work at a higher chopping frequency or a lower sampling rate. In theory, we could sample at the Nyquist frequency (for this work, at 150 kHz) without any ill effects. Moreover, chopping at a higher frequency has several potential benefits: a higher data throughput, and reduced contribution of  $1/f$  noise. Fitting regimes work best when they have several ringdown lengths worth of data to analyse [8]; this limits the rate at which one can generate data. Our method does not have this restriction. Our method is very easy to code; the section of the matlab script that does the analysis is only four lines long. This simplicity should make implementation on an FPGA feasible; this could result in even greater speed gains, and the possibility for real time analysis. Because our method is based in the frequency domain, the acquisition electronics are much easier to design: we could AC couple the ringdown signal with no ill effects. This is convenient as many high speed digitisers only have AC coupled inputs. We have locked our cavity with a simple analog PI controller. We are presently investigating using modern control theory [12] to improve the quality of the lock between the laser and the cavity. The quality of the lock is directly related to the precision of the instrument. If we can increase the bandwidth of the controller, we can better counteract perturbations over a wider frequency range. This will reduce the amount of noise present on the ringdown waveform.

## 6. Conclusions

In this paper, we have proposed a new method for analysing the output of a CW Cavity ring-down spectrometer; our method analyses the output of the spectrometer as a whole, rather than just analysing individual ringdown transients. We have simulated the technique, comparing it to Levenburg-Marquardt non-linear least squares fitting, and used a modelocked CRDS instrument that we have built for proof-of-principle tests. Our method greatly simplifies the design of acquisition electronics. We have found that our method has a comparable accuracy, and comparable or higher precision, to LM, but analyses data 500 times faster.

## Acknowledgments

We would like to thank the Australian Research Council, the Australian Federal Police, the Defence and Security Applications Research Centre, the National Science Foundation, and the Louisiana Board of Regents for their support of this research.

# Nonlinear estimation of ring-down time for a Fabry-Perot optical cavity

Abhijit G. Kallapur,\* Toby K. Boyson, Ian R. Petersen,  
and Charles C. Harb

School of Engineering and Information Technology,  
University of New South Wales at the Australian Defence Force Academy,  
Canberra, ACT, 2600, Australia

[\\*abhijit.kallapur@gmail.com](mailto:abhijit.kallapur@gmail.com)

**Abstract:** This paper discusses the application of a discrete-time extended Kalman filter (EKF) to the problem of estimating the decay time constant for a Fabry-Perot optical cavity for cavity ring-down spectroscopy (CRDS). The data for the estimation process is obtained from a CRDS experimental setup in terms of the light intensity at the output of the cavity. The cavity is held in lock with the input laser frequency by controlling the distance between the mirrors within the cavity by means of a proportional-integral (PI) controller. The cavity is purged with nitrogen and placed under vacuum before chopping the incident light at 25KHz and recording the light intensity at its output. In spite of beginning the EKF estimation process with uncertainties in the initial value for the decay time constant, its estimates converge well within a small neighborhood of the expected value for the decay time constant of the cavity within a few ring-down cycles. Also, the EKF estimation results for the decay time constant are compared to those obtained using the Levenberg-Marquardt estimation scheme.

© 2011 Optical Society of America

**OCIS codes:** (300.6360) Laser spectroscopy; (050.2230) Fabry-Perot; (200.3050) Information processing.

---

## References and links

1. A. O'Keefe and D. A. G. Deacon, "Cavity Ring-Down Optical Spectrometer for Absorption Measurements using Pulsed Laser Sources," *Rev. Sci. Instrum.* **59**, 2544–2551 (1988).
2. B. A. Paldus, C. C. Harb, T. G. Spence, B. Wilke, J. Xie, J. S. Harris, and R. N. Zare, "Cavity-Locked Ring-Down Spectroscopy," *J. Appl. Phys.* **83**, 3991–3997 (1998).
3. K. W. Busch and M. A. Busch, *Cavity-Ringdown Spectroscopy. An Ultratrace-Absorption Measurement Technique*, vol. 720 of *ACS Symposium Series* (American Chemical Society, Washington, DC, 1999).
4. T. G. Spence, C. C. Harb, B. A. Paldus, R. N. Zare, B. Willke, and R. L. Byer, "A Laser-Locked Cavity Ring-DOWN Spectrometer Employing an Analog Detection Scheme," *Rev. Sci. Instrum.* **71**, 347–353 (2000).
5. J. Xie, B. A. Paldus, E. H. Wahl, J. Martin, T. G. Owano, C. H. Kruger, J. S. Harris, and R. N. Zare, "Near-Infrared Cavity Ringdown Spectroscopy of Water Vapor in an Atmospheric Flame," *Chem. Phys. Lett.* **284**, 387–395 (1998).
6. A. A. Istratov and O. F. Vyvenko, "Exponential analysis in physical phenomena," *Rev. Sci. Instrum.* **70** 1233 (1999).
7. M. Mazurenka, R. Wada, A. J. L. Shillings, T. J. A. Butler, J. M. Beames, and A. J. Orr-Ewing, "Fast fourier transform analysis in cavity ring-down spectroscopy: application to an optical detector for atmospheric NO<sub>2</sub>," *Appl. Phys. B: Lasers Opt.* **81**, 135–141 (2005).
8. M. A. Everest and D. B. Atkinson, "Discrete Sums for the Rapid Determination of Exponential Decay Constants," *Rev. Sci. Instrum.* **79**, 023108–023108–9 (2008).
9. C. K. Chui and G. Chen, *Kalman Filtering with Real-Time Applications*, Theoretical, Mathematical & Computational Physics (Springer-Verlag, Berlin, Heidelberg, Germany, 2009), 4th ed.

10. A. G. Kallapur, I. R. Petersen, T. K. Boyson, and C. C. Harb, "Nonlinear Estimation of a Fabry-Perot Optical Cavity for Cavity Ring-Down Spectroscopy," in "IEEE International Conference on Control Applications (CCA)," (Yokohama, Japan, 2010), pp. 298–303.
11. S. Z. Sayed Hassen, E. Huntington, I. R. Petersen, and M. R. James, "Frequency Locking of an Optical Cavity Using LQG Integral Control," in "17th IFAC World Congress," (Seoul, South-Korea, 2008), pp. 1821–1826.
12. S. Z. Sayed Hassen, M. Heurs, E. H. Huntington, I. R. Petersen, and M. R. James, "Frequency Locking of an Optical Cavity using Linear-Quadratic Gaussian Integral Control," *J. Phys. B: At. Mol. Opt. Phys.* **42**, 175501 (2009).
13. S. Z. Sayed Hassen and I. R. Petersen, "A time-varying Kalman filter approach to integral LQG frequency locking of an optical cavity," in "American Control Conference," (Baltimore, MD, USA, 2010), pp. 2736–2741.
14. C. W. Gardiner and P. Zoller, *Quantum Noise* (Springer, Berlin, Germany, 2000).
15. H. A. Bachor and T. C. Ralph, *A Guide to Experiments in Quantum Optics* (Wiley-VCH, Weinheim, Germany, 2004), 2nd ed.
16. R. W. P. Drever, J. L. Hall, F. V. Kowalski, J. Hough, G. M. Ford, A. J. Munley, and H. Ward, "Laser Phase and Frequency Stabilization using an Optical Resonator," *Appl. Phys. B: Lasers Opt.* **31**, 97–105 (1983).

## 1. Introduction

Cavity ring-down spectroscopy (CRDS) is a cavity enhanced spectroscopic technique that works by injecting tunable coherent light from a laser or a nonlinear optical device either pulsed or continuous-wave into a resonant optical cavity containing two or more highly reflective mirrors. The optical cavity contains the field, and allows for a long effective pathlength (typically of the order of kilometers), thus intensifying the measurement of photon loss inside the cavity as a function of the optical wavelength; e.g., see [1–4]. In this paper, we consider a Fabry-Perot optical cavity consisting of a hollow tube fitted with two highly reflective mirrors. When the input laser frequency matches the resonant frequency of the cavity, it is said to be in *lock* with the cavity. Any deviation between these frequencies is characterized in terms of the *detuning parameter*  $\Delta$  and is an undesired effect.

If the light coupling into the cavity is interrupted, light inside the cavity continues to resonate and gradually decays in intensity. This intensity information is recorded to study the decay of light inside the cavity as a function of wavelength. The time taken for the light intensity to decay to  $1/e$  times its initial value is termed as the decay time  $\tau$ . This decay time depends upon the reflectivity of the mirrors mounted inside the cavity and losses due to the sample contained within the cavity which directly dictates the amount of optical absorption or scatter. Hence, an estimate of  $\tau$  in such a spectroscopic technique can be used as a molecular detector in chromatographic systems and for applications in molecular fingerprinting which involves detecting various chemicals, such as explosives and their related compounds.

Conventional linear least square techniques can be used to estimate the value for  $\tau$  if the logarithm of the decay of the cavity field is considered [1, 5]. However, linear methods are applied to estimate  $\tau$  in the case of isolated ring-downs and are susceptible to system noise characteristics and instrument offsets; e.g., see [6, 7]. On the other hand, nonlinear least square methods such as the Levenberg-Marquardt (LM) algorithm can handle system noise more effectively but is known to limit the data throughput to below 10Hz [8]. In order to overcome these issues and considering the underlying system dynamics to be linear, an optimal estimator such as the linear Kalman filter (KF) can be employed, which has been successfully used for real-time estimation in various fields; see e.g., [9]. However, in our case, since the measurement involves output light intensity, which is a nonlinear function of the magnitude and phase quadratures, we need to consider nonlinear estimation schemes with real-time implementation capabilities and better throughput than the LM method. To this effect, we propose the use of the extended Kalman filter (EKF) which is the nonlinear counterpart of the linear KF. It was shown in simulation in [10] that the EKF could be used to estimate the states (magnitude and phase quadratures) and parameters ( $\tau$  and  $\Delta$ ) for a Fabry-Perot optical cavity. In this paper, we

apply the EKF to estimate  $\tau$  for a set of experimentally obtained output intensity data for a Fabry-Perot optical cavity. During the course of the experiment,  $\Delta$  was maintained near zero with the aid of a proportional-integral (PI) controller which was used to maintain the distance between the two mirrors inside the cavity so as to match the cavity's resonant frequency with the input laser frequency. Also, the EKF estimation results for  $\tau$  are compared to those obtained by applying the LM technique to the same set of ring-down data.

The rest of the paper is organized as follows: Section 2 explains the basics of the CRDS technique using a Fabry-Perot optical cavity and introduces the application of modern estimation and control techniques to such an optical system. Section 3 provides a detailed description of a continuous-time mathematical model describing the dynamics for the optical cavity in terms of amplitude and phase quadratures. It also reformulates these dynamics in terms of a state-space representation. A brief introduction to the discrete-time EKF and its recursion equations are presented in Section 4. This section also describes the conversion of the continuous-time state-space equations of Section 3 into their discrete-time counterparts which are used to estimate the value of the decay time constant ( $\tau$ ). A detailed description of the experimental setup and the estimation results for  $\tau$  are presented in Section 5 with a comparison between EKF estimation results and LM estimation results. Finally, conclusions and a note on future work are outlined in Section 6.

## 2. Estimation and control for cavity ring-down spectroscopy

Consider the block diagram in Fig. 1 representing an application of modern estimation and control techniques to a CRDS setup. This block diagram can be grouped into two parts: The first

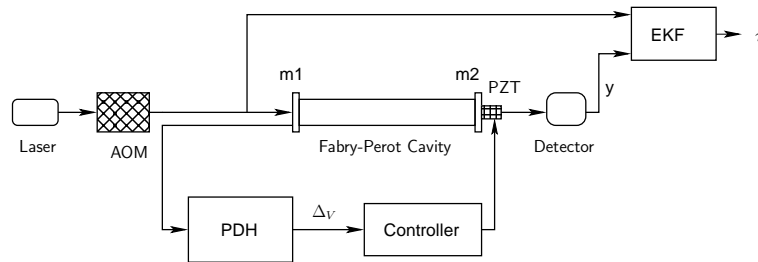


Fig. 1. Proposed CRDS setup with an EKF estimator and a controller.

part is a CRDS setup comprising of a laser, an acousto-optical modulator (AOM) and a Fabry-Perot optical cavity; and the second part consists of an estimation-control loop comprising of an EKF and a controller. As mentioned in Section 1, light is coupled to the Fabry-Perot cavity via a fast optical switch such as an AOM. Considering the cavity to be locked, that is, the laser frequency is the same as the resonant frequency of the cavity, the light intensity inside the cavity builds due to constructive interference. When light coupling to the cavity is interrupted, its intra-cavity intensity slowly decays depending upon the absorption properties of absorbing species in the cavity as well as the reflectivity of the mirrors within the cavity. This effect is termed as the *ring-down* effect. Indeed, the ring-down time or decay time ( $\tau$ ), which is the time taken for the light inside the cavity to decay to  $1/e$  of its original intensity, can be computed, which gives a good indication of the absorptive losses associated with the cavity.

Traditional data processing techniques for CRDS focus on fitting each individual decay curve to an exponential equation described by,

$$I(t) = I_0 \exp\left(-\frac{t}{\tau}\right), \quad (1)$$

where  $I(t)$  represents the decay amplitude at time  $t$ ,  $I_0$  is the initial intensity of the field within the cavity, and  $\tau$  is the decay time constant. Indeed, the decay time is a direct measure of losses within the cavity and can be described as,

$$\tau = \frac{t_{rt}}{c \varepsilon(\lambda) + n(1-R) + \alpha}, \quad (2)$$

where  $t_{rt}$  is the round-trip time for light within the cavity,  $\varepsilon(\lambda)$  is the extinction coefficient of an absorbing species with concentration  $c$  computed as a function of the wavelength ( $\lambda$ ) of the incident light on the cavity. Also,  $n$  is the number of mirrors with reflectivity  $R$  and  $\alpha$  is a lumped term comprising of other absorptions.

The CRDS technique either requires that decay be linearized and a linear least squares fit applied, or that a nonlinear least squares algorithm, usually Levenberg-Marquardt (LM), be employed. Though such techniques accurately determine  $\tau$  for CRDS, they are slow [8]. Also, if the data is noisy, which is generally the case for a simple pulsed system, tens or hundreds of ring-down times may need to be acquired and averaged in order to obtain an accurate result. However, in some applications, it is required that the estimation of  $\tau$  occur in real-time. Since the decaying light intensity as seen at the output of the cavity is a nonlinear function of the magnitude and phase quadratures, we need a suitable nonlinear estimator to estimate  $\tau$ . Hence, we propose the use of an extended Kalman filter (EKF), which is a suboptimal nonlinear estimator, in order to determine  $\tau$ .

For the ring-down estimation to be accurate, the deviation of input laser frequency from the cavity's resonant frequency characterized by the *detuning parameter*  $\Delta$ , needs to be maintained at zero. In other words, cavity lock should be maintained. This can be achieved by varying the length between the two mirrors, m1 and m2, in the Fabry-Perot cavity by means of a piezoelectric actuator (PZT), controlled using a suitable controller (see Fig. 1). As mentioned in Section 1, this process varies the length of the cavity, hence affecting its resonant frequency. As shown in the Fig. 1, one way to achieve this is by recording the light intensity at the reflected port of the cavity and using the Pound-Drever-Hall (PDH) method to obtain an analogue voltage ( $\Delta_V$ ) proportional to  $\Delta$ . This information is then used by the controller to position mirror m2 via a PZT to maintain cavity lock.

In this paper, we will discuss the application of a discrete-time EKF to estimate the decay-time for a set of experimentally obtained intensity data for a frequency-locked Fabry-Perot optical cavity. The cavity was held in lock with the input laser frequency using a PI controller. Though modern control theory such as linear Gaussian (LQG) control [11–13] and other  $H_2/H_\infty$  control methods can be used to improve locking in the presence of noise and uncertainties, they will not be considered in the scope of this paper. A description of the cavity dynamics in terms of a state-space representation follows.

### 3. Cavity dynamics

Consider the following set of continuous-time equations describing the dynamics of the optical cavity; e.g, see [14, 15]:

$$\dot{a} = -\left(\frac{\gamma}{2} + i\Delta\right)a - \sqrt{\gamma_m}(\bar{a}_m + w), \quad (3)$$

$$y = \gamma_m a^\dagger a + v. \quad (4)$$

Here,  $a$  denotes the annihilation operator for the cavity mode defined in an appropriate rotating frame,  $(\cdot)^\dagger$  represents the operator adjoint operation,  $\gamma = \gamma_m + \gamma_c$  is the total cavity coupling coefficient.  $\gamma_m$  represents the cavity coupling coefficient at the mirrors in a vacuum cavity and  $\gamma_c$  represents the cavity coupling coefficient corresponding to the absorbers within the cavity.

Also,  $\Delta$  is the detuning parameter,  $\bar{a}_{in}$  the laser input,  $y$  is the measured output corresponding to the output light intensity, and  $w$  and  $v$  represent lumped process and measurement noise terms respectively.

We then define quadrature variables for amplitude ( $q$ ) and phase ( $p$ ) in terms of the annihilation operator ( $a$ ) as,

$$q = a + a^\dagger; \quad p = \frac{a - a^\dagger}{i} \quad (5)$$

which upon time-differentiation gives,

$$\dot{q} = \dot{a} + \dot{a}^\dagger; \quad \dot{p} = \frac{\dot{a} - \dot{a}^\dagger}{i}. \quad (6)$$

In order to obtain the cavity dynamics in terms of quadrature components, we begin by substituting (3) into (6). This gives,

$$\begin{aligned} \dot{q} &= -\frac{\gamma}{2}(a + a^\dagger) - i\Delta(a - a^\dagger) - 2\sqrt{\gamma_m}\bar{a}_{in} - \sqrt{\gamma_m}(w + w^\dagger), \\ &= -\frac{\gamma}{2}q + \Delta p - 2\sqrt{\gamma_m}\bar{a}_{in} - \sqrt{\gamma_m}w_q, \end{aligned} \quad (7)$$

$$\begin{aligned} \dot{p} &= -\frac{\gamma}{2}\left(\frac{a - a^\dagger}{i}\right) - \Delta(a + a^\dagger) - \sqrt{\gamma_m}\left(\frac{w - w^\dagger}{i}\right), \\ &= -\frac{\gamma}{2}p - \Delta q - \sqrt{\gamma_m}w_p, \end{aligned} \quad (8)$$

where,  $w_q = w + w^\dagger$  and  $i w_p = w - w^\dagger$ . Considering the time dependence of various terms and writing (7) and (8) in the state-space form, we get,

$$\begin{bmatrix} \dot{q}(t) \\ \dot{p}(t) \end{bmatrix} = \begin{bmatrix} -\gamma/2 & \Delta \\ -\Delta & -\gamma/2 \end{bmatrix} \begin{bmatrix} q(t) \\ p(t) \end{bmatrix} - \sqrt{\gamma_m} \begin{bmatrix} 1 & 1 & 0 \\ 0 & 0 & 1 \end{bmatrix} \begin{bmatrix} 2\bar{a}_{in} \\ w_q(t) \\ w_p(t) \end{bmatrix} \quad (9)$$

which is in the state-space form,

$$\dot{\bar{x}}(t) = A_c \bar{x}(t) + B_c \bar{u}(t) + D_c \bar{w}(t), \quad (10)$$

where  $\bar{x}(t) = [q(t), p(t)]^T$  is the state vector,  $\bar{u}(t) = 2\bar{a}_{in}$  is the input to the system, and  $\bar{w}(t) = [w_p(t), w_q(t)]$  is the lumped quadrature noise vector. Also,  $A_c$ ,  $B_c$ , and  $D_c$  are given matrices. In the sequel, the system (9) will be treated as a classical state-space system.

Similarly, the nonlinear output dynamics (4) can also be written in terms of the state vector as,

$$y(t) = h(x(t)) + v(t), \quad (11)$$

where the nonlinear function  $h(x(t)) = \frac{\gamma_m}{4}(q(t)^2 + p(t)^2)$  and  $v(t)$  is the lumped measurement noise.

#### 4. EKF recursion and design

The linear Kalman filter (KF) is an optimal minimum mean-square estimator. It combines the expected value of measurements of a system in terms of dynamic (mathematical) models with noisy measurements usually obtained from sensor(s) to provide values closer to the true measurement. Indeed, such an optimal filter can be applied to linear systems only. In the case of nonlinear systems with nonlinear dynamics, measurements or both, the system equations can

be linearized about the current operating point or estimated trajectory and the recursion equations of the linear KF are applied to the resulting linearized system equations. This extension of the KF to nonlinear systems is known as the extended Kalman filter (EKF) and is a suboptimal variant of its linear counterpart. As seen from (11), the measurement equation describing the intensity of light at the output of the cavity is a nonlinear function of the quadrature states  $q$  and  $p$ . The estimation of states in this case requires the application of a nonlinear filter such as the EKF which is described in the rest of this section. Also, since the measurements are obtained at discrete intervals of time, we shall apply the recursion equations of a discrete-time EKF.

Consider a nonlinear discrete-time system with the following dynamics,

$$x_k = f(x_k, u_k) + w_k, \quad (12)$$

$$y_{k+1} = h(x_{k+1}) + v_{k+1}, \quad (13)$$

where  $x_{(\cdot)} \in \mathbb{R}^n$  is the state,  $u_{(\cdot)} \in \mathbb{R}^m$  is the known input,  $w_{(\cdot)} \in \mathbb{R}^p$  and  $v_{(\cdot)} \in \mathbb{R}^q$  are the process and measurement noise inputs respectively, and  $y_{(\cdot)} \in \mathbb{R}^l$  is the measured output. Also,  $f(\cdot)$  and  $h(\cdot)$  are given nonlinear functions. For the system described in (12) - (13), the EKF *propagation* and *update* recursion equations are given by,

#### Propagation

$$x_{k+1}^- = f(x_k^+, u_k) \quad (14)$$

$$P_{k+1}^- = F_k P_k^+ F_k^T + Q \delta. \quad (15)$$

#### Update

$$K_{k+1} = P_{k+1}^- H_{k+1}^T (H_{k+1} P_{k+1}^- H_{k+1}^T + R)^{-1}, \quad (16)$$

$$x_{k+1}^+ = x_{k+1}^- + K_{k+1} (y_{k+1} - h(x_{k+1}^-)), \quad (17)$$

$$P_{k+1}^+ = I - K_{k+1} H_{k+1} P_{k+1}^-. \quad (18)$$

Here, the *propagation* step consists of estimating the value of the state  $x$  and covariance  $P$  (a matrix representing the approximate variance of the estimate of the state from its true value) one time-step ahead. These values are computed using available state(s) and input(s) at the current time-step and evaluating the state dynamics  $f(x_k^+, u_k)$ . The errors in propagation are then corrected using the measured sensor value(s) in the *update* step. Also, in (14) - (18),  $y_{(\cdot)}$  is the measured sensor output and  $F_{(\cdot)}$ ,  $H_{(\cdot)}$  are the linearized process and output matrices respectively, computed about the current operating point as,

$$F_k = \left. \frac{\partial f(x, u)}{\partial x} \right|_{x=x_k^+}; \quad H_{k+1} = \left. \frac{\partial h(x)}{\partial x} \right|_{x=x_{k+1}^-}. \quad (19)$$

In addition,  $K(\cdot)$  represents the Kalman gain,  $P$  is the covariance matrix,  $Q$  and  $R$  are the process and measurement noise matrices, and  $I$  is the identity matrix of suitable dimensions. Also,  $(\cdot)^-$  and  $(\cdot)^+$  represent apriori and posteriori values respectively; and  $\delta$  is the sampling time constant.

Since we are interested in estimating the value for  $\tau (= 1/\gamma)$ , the continuous-time linear model in (9) is written in the following form,

$$\begin{aligned} \dot{x}(t) &= \tilde{A}_c x(t) + \tilde{B}_c u(t) + \tilde{D}_c(t) w(t), \\ &= \begin{bmatrix} -\gamma(t)/2 & \Delta(t) & 0 \\ -\Delta(t) & -\gamma(t)/2 & 0 \\ 0 & 0 & 0 \end{bmatrix} \begin{bmatrix} q(t) \\ p(t) \\ \gamma(t) \end{bmatrix} + \begin{bmatrix} -\sqrt{\gamma_m} \\ 0 \\ 0 \end{bmatrix} 2\bar{a}_{in} + \sqrt{\gamma_m} \begin{bmatrix} -1 & 0 \\ 0 & -1 \\ 0 & 0 \end{bmatrix} \begin{bmatrix} w_q(t) \\ w_p(t) \\ 0 \end{bmatrix} \end{aligned} \quad (20)$$

where,  $x(t) = [q(t), p(t), \gamma(t)]^T$  is the *augmented state vector* with the dynamics for the constant term  $\gamma (= 1/\tau)$  added to the original state vector  $\bar{x}$  defined in (10). The nonlinear measurement equation, however, remains the same as in (11).

In order to apply the discrete-time EKF recursion equations, the continuous-time model presented in (20) and (11) needs to be written in the corresponding discrete-time format. This transformation is achieved as,

$$f(x_k, u_k) = A_d x_k + B_d u_k, \quad (21)$$

where,

$$A_d = e^{[\bar{A}_c \cdot \delta]}; \quad B_d = \int_0^\delta \left\{ e^{[\bar{A}_c \cdot s]} ds \cdot \bar{B}_c \right\} \quad (22)$$

and

$$D_d = \int_0^\delta \left\{ e^{[\bar{A}_c \cdot s]} ds \cdot \bar{D}_c \right\} \quad (23)$$

with  $\delta$  the sampling time. Also, the discrete-time measurement equation is computed as,

$$y_{k+1} = h(x_{k+1}) + v_{k+1} = \frac{\gamma_m}{4} (q_{k+1}^2 + p_{k+1}^2) + v_{k+1}. \quad (24)$$

The actual estimation process comprised of the application of the discrete-time EKF recursion Eqs. (14)-(18) to the light intensity data captured at the output of the cavity. For this purpose, various matrices and constants defined in Eqs. (14)-(18) were set as follows:

$$Q = \begin{bmatrix} 0.171 \times 10^{-12} & 0 & 0 \\ 0 & 0.171 \times 10^{-12} & 0 \\ 0 & 0 & 0 \end{bmatrix}; \quad R = 2 \times 10^{-10}. \quad (25)$$

Since the cavity was purged with nitrogen and placed under vacuum before recording the intensity data at its output, most of the losses within the cavity were due to the mirrors. Hence,  $\gamma_m \gg \gamma_c$ , which meant that  $\tau$  was almost equal to the decay time constant for an empty cavity. Considering the reflectivity of mirrors used in the experiment (explained in Section 5), the value of  $\tau$  for the cavity was expected to be around  $5.26 \mu\text{s}$ , corresponding to  $\gamma = 1.9 \times 10^5$ . This was used as an indication for the approximate true value for  $\tau$  during the estimation process. In accordance, the initial state vector  $[q_0, p_0, \gamma_0]^T$  representing initial values for the amplitude quadrature, the phase quadrature and the total cavity coupling coefficient were set to  $[0, 0, 1.805 \times 10^5]^T$ . Here,  $\gamma_0$  was set with a 5% error from its expected true value of  $1.9 \times 10^5$ . Also, the corresponding covariance matrix  $P$  reflecting error variance in initial conditions was set to,

$$P_0 = \begin{bmatrix} 0.171 \times 10^{-12} & 0 & 0 \\ 0 & 0.171 \times 10^{-12} & 0 \\ 0 & 0 & 10^9 \end{bmatrix}. \quad (26)$$

The output intensity measurements were collected into the vector  $y_{(\cdot)}$  defined in (24) and the sampling time constant  $\delta$  was set to  $10^{-8}$ s.

A detailed description of the experimental setup and EKF estimation results are presented in the next section.

## 5. Experimental setup and results

A block diagram describing the experimental setup used to collect ring-downs from a Fabry-Perot cavity is depicted in Fig. 2. Light from an external cavity tunable diode laser (New Focus

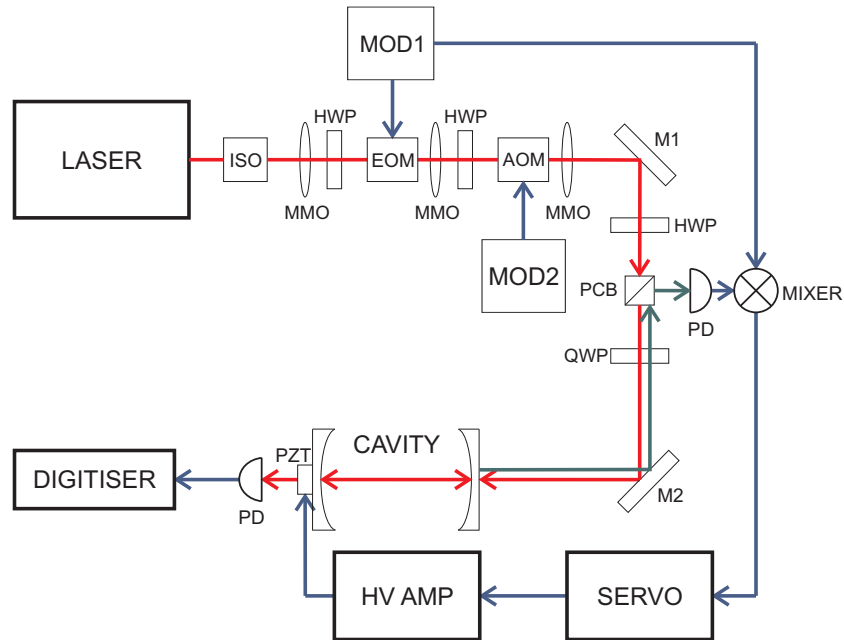


Fig. 2. Block diagram of CRDS experimental setup: The red and green lines represent optical signal paths whereas the blue line represents the path for electronic signals. Also, ISO is the Faraday isolator; MMO are mode matching optics; HWP are half wave plates; EOM is the electro-optic modulator; AOM is the acousto-optic modulator; MOD1 is the RF generator and amplifier for phase modulation; MOD2 is the signal generator and amplifier used to generate the chopping waveform; M1 and M2 are beam steering mirrors; PCB is a polarizing cube beamsplitter; PD are photodetectors; QWP is a quarter wave plate; SERVO is the controller; HV AMP is a  $\pm 200V$  amplifier to drive PZT, the piezoelectric actuator that controls the cavity length.

6330, 10mW tunable from 1540-1640 nm) is passed through a Faraday isolator in order to prevent unwanted optical feedback. The light is then passed through an electro-optic modulator (EOM) (Thorlabs). The EOM places FM sidebands (at  $\pm 18.5$  MHz) on the laser radiation; these are used to lock the cavity to the laser using the method outlined in [16]. The phase modulated light is then passed through an Acousto-Optic Modulator (AOM) (Brimrose) that is used to rapidly switch the laser light on and off (at 25KHz for this experiment), generating a square waveform. The light then passes through a polarizing cube beamsplitter (PCB) and a quarter wave plate (QWP) before entering the optical cavity. The reflected beam passes back through the optical circulator, and is tapped off to lock the cavity. The cavity is a stainless steel tube (Los Gatos Research) with 99.96% mirrors as both the input and output couplers (Advanced Thin Films,  $R > 99.96\%$ , loss  $< 10\text{ppm}$ ). These mirrors give a calculated empty cavity ring-down time of  $\approx 5\mu\text{s}$ . Both reflected and transmitted photodetectors were designed and built in-house and have a 3 dB bandwidth  $> 20\text{MHz}$ . The cavity is locked with an in-house designed analog PI controller with a unity gain bandwidth of 1KHz. Light exiting the cavity is acquired using a high-speed digitizing oscilloscope (Clevscope 3284A, 100MS/sec, 14 bits), and exported to Matlab<sup>®</sup> for estimating the value for  $\tau$ . Twenty ring-down cycles of this data were used for the estimation process, with Fig. 3 depicting a sample ring-up and ring-down cycle.

In order to estimate the ring-down time constant, the discrete-time EKF recursion Eqs. (14)-

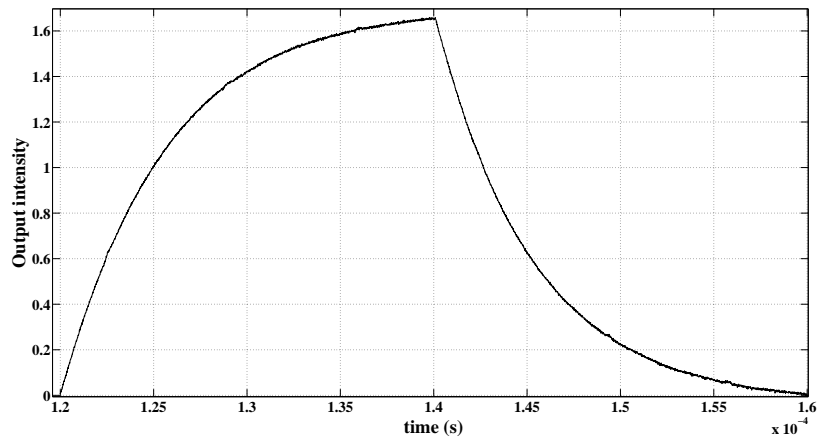


Fig. 3. Sample light intensity data obtained at the output of the cavity.

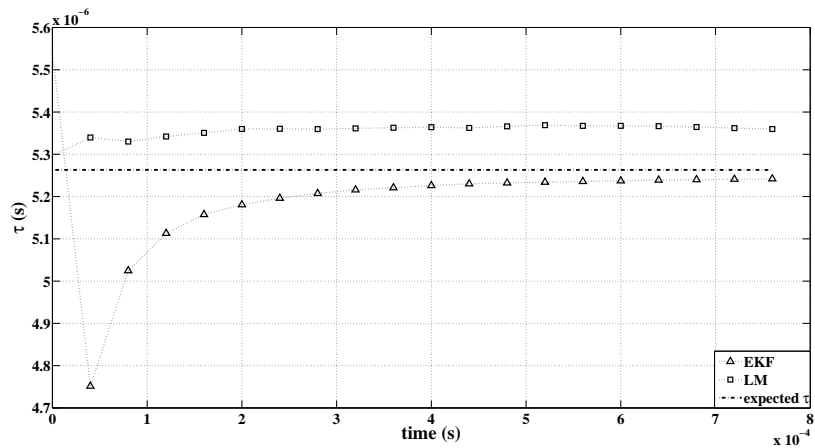


Fig. 4. A comparison of EKF and LM estimation results for  $\tau$  at the end of each ring-down cycle, plotted against the expected true value for  $\tau$ .

(18) and associated constants and matrices outlined in Section 4 were applied to the light intensity data captured at the output of the cavity. This estimation process took about  $1.4s$  for one cycle of ring-up and ring-down data. Since the EKF is a suboptimal method, its estimates converge to a neighborhood of the expected true value for  $\tau$  at  $5.26\mu s$  and oscillate with a variation of  $\pm 0.012\mu s$ . In addition, the LM technique was also applied to the recorded intensity data and the estimation results for the ring-down time were compared to that obtained from the EKF at the end of each ring-down cycle. This is depicted in Fig. 4. As seen from Fig. 4, EKF estimates converge to a small neighborhood of the expected true value for  $\tau$  whereas the LM estimates converge to within  $0.1\mu s$  of the expected true value for  $\tau$  at the end of 19 ring-down cycles.

Another advantage of the EKF is in the number of ring-down cycles needed to converge to a neighborhood of the expected true value for  $\tau$ . Since the EKF is a recursive method and relies on the states and parameters at the previous instant in time to estimate the corresponding states and parameters at the current time instant by propagating these values through the

system dynamical Eqs. (20)-(23). The associated estimation error improves with time as successive measurements are obtained and the filter recursion is carried out until the estimate for the state(s) converges to a certain neighborhood of the expected true state. This is a direct consequence of the large deviation of the EKF estimated values for  $\tau$  during the initial few cycles as depicted in Fig. 4, after which the error in estimation gradually reduces and the estimate settles within a neighborhood of the expected true value for  $\tau$ . On the other hand, in the case of the curve-fitting LM method, every ring-down cycle is considered independently of the previous cycle and the value for  $\tau$  is estimated separately for each ring-down cycle. This is why the LM algorithm generally needs hundreds of ring-down cycles to obtain an acceptable value for  $\tau$  after averaging the statistics obtained at the end of each ring-down cycle, which is not the case with the EKF.

## 6. Conclusion

The application of a discrete-time extended Kalman filter (EKF) for the estimation of the decay time constant for cavity ring-down spectroscopy was presented. The experimental setup consisted of a Fabry-Perot optical cavity which was purged with nitrogen and placed under vacuum before recording the light intensity at its output, which was then exported to Matlab<sup>®</sup> for the estimation process. Since the cavity was almost empty during the process of data accumulation, the losses in the cavity were mainly due to the mirrors, with very little or no effect due to other factors contributing to the absorption or scattering of light within the cavity. Hence, the approximate value for  $\tau$  in the estimation process was expected to be close to that of an empty cavity. Considering the reflectivity of mirrors used in the experiment, the value for  $\tau$  of the cavity was expected to be around  $5.26\mu s$  (corresponding to  $\gamma = 1.9 \times 10^5$ ).

The EKF was applied to the output intensity data obtained from the cavity after locking the cavity to the input laser frequency via a PI controller. The (mathematical) dynamics for the cavity were set in terms of its amplitude and phase quadratures and the recursion equations of the discrete-time EKF were used for the estimation process. The EKF estimates for  $\tau$  converged to the neighborhood of the expected true value of  $5.26\mu s$  within a few cycles of the output ring-down data. The Levenberg-Marquardt (LM) technique was also implemented and its estimation results were compared to that of the EKF at the end of each ring-down cycle. It was found that the LM estimate for  $\tau$  had a  $0.1\mu s$  deviation from the expected true value for  $\tau$  at the end of 19 ring-down cycles, whereas the EKF converged to a neighborhood of the expected true value for  $\tau$  oscillating with a variation of  $0.012\mu s$  after the same number of ring-down cycles.

Indeed, the estimation time can be improved by using a subset of the intensity data points whereas the accuracy of results can be improved by considering the effect of unmodeled dynamics for the cavity model. We are currently working on applying the EKF to the estimation of  $\tau$  in real-time using field programmable gate arrays (FPGA).

## Acknowledgments

This work was supported by the Australian Research Council.